THE ENERGY RESOLUTION FUNCTION FOR THE CAMEA NEUTRON SPECTROMETER

PROJECT OUTSIDE OF THE COURSE SCOPE

Written by *Kristine M. L. Krighaar (rqw129)*

November 24, 2021

Supervised by
Kim Lefmann

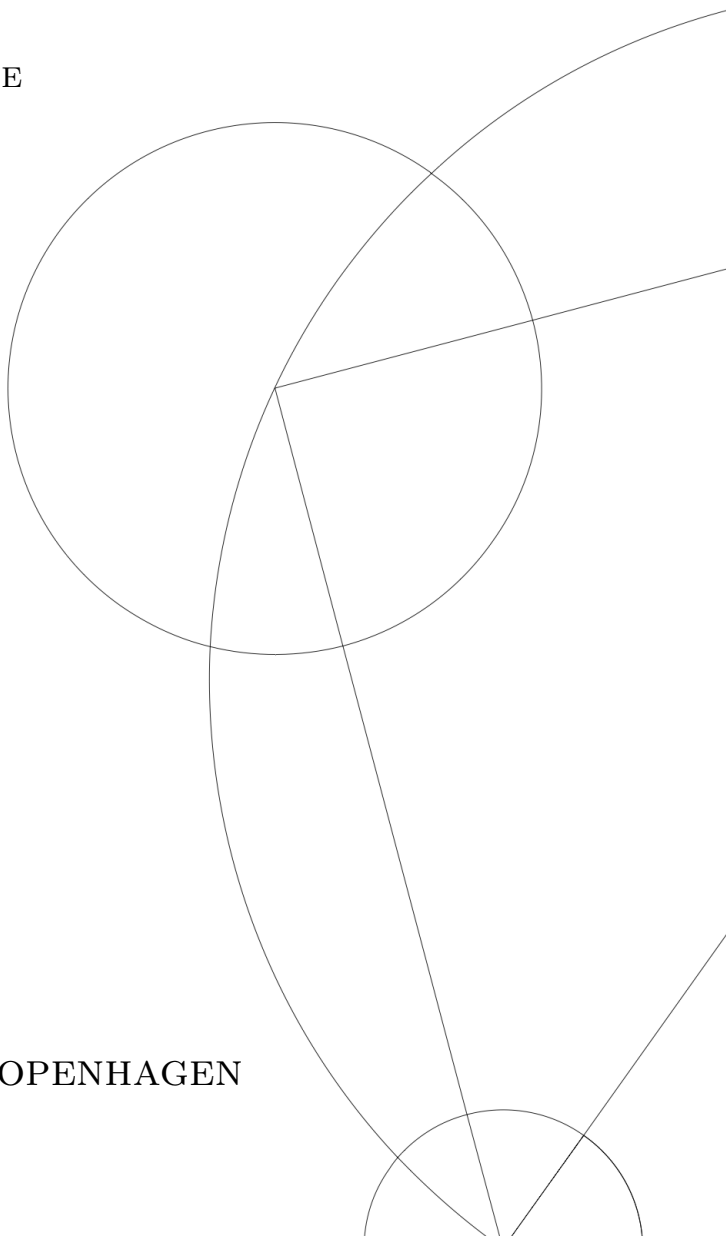

UNIVERSITY OF COPENHAGEN

UNIVERSITY OF COPENHAGEN

Name of Institute:	Niels Bohr Institutet
Name of Department:	Condensed Matter Physics
Author(s):	Kristine M. L. Krighaar (rqw129)
Email:	kristine.krighaar@nbi.ku.dk

Title and subtitle:	the energy resolution function for the CAMEA neutron spectrometer -
Supervisor(s):	Kim Lefmann
Handed in:	24.11.2021

Abstract

This project deals with simulating the elastic energy resolution function of the CAMEA triple axis neutron spectrometer, located at PSI in Switzerland, using the Monte Carlo ray-tracing package McStas. First an introduction is made to scattering theory and the setup of the CAMEA instrument is explained, as well as some of the instrumentation techniques it utilizes, such as the prismatic analyzer concept. The methods used to determine the resolution function is explained to give insight into how the McStas model works and multiple different tests are performed with the simulation model both for validation and to investigate features about the CAMEA instrument showing that the simulation model is highly useful furthering understanding of the CAMEA instrument.

Acknowledgements

Thanks to my supervisor Kim Lefmann for the help with the project and for help arranging for me to go to Switzerland and work with the CAMEA team.

Thanks to the CAMEA instrument team Christof, Daniel, Elizabetta and Jakob, for giving me the opportunity to let me come and join you for two months and teaching me a lot about practical neutron scattering. A special thanks to Jakob for all the amazing help with the project.

Contents

1 Introduction

Triple axis spectrometers (TAS) is a class of highly versatile neutron scattering instruments that enables measurements of inelastic signals in single crystal materials. By being able to measure inelastic scattering; TAS can be used for determining dynamic and magnetic properties of crystalline materials, by measuring magnon and phonon dispersions under a number of different conditions such as temperature, pressure or magnetic field [1]. Since the fist TAS build by Brockhouse at Chalk River Laboratories[2], decades worth of development has improved these instruments, so that not only can measurement be performed faster, and we are able to get more precise results.

The Continuous Angle Multiple Energy Analysis (CAMEA) spectrometer[3] is a new type of TAS that measures multiple points in reciprocal space at multiple energies all at once, known as a multiplexing TAS instrument. This allows for wider ranging measurements collected at a fraction of the time than what was possible previously. This is especially true after the resent improvements in neutron flux on the instrument, with the acquirement and instalments of a new doubly focusing monochromator.

Since CAMEA is a new kind of TAS that applies many new techniques such as the prismatic analyzer concept, multiplexing and upward out of plane scattering[4], little is known about the effects on the energy resolution of these types of multiplexing instruments. CAMEA is not the only of its kind, the MultiFLEXX[5] and the future BIFROST instrument at ESS [6] also utilizes these principles. This project therefore focuses on how the energy resolution behaves specifically for the CAMEA instrument. This is done through simulation with the ray tracing Monte-Carlo program McStas[7] and compares the simulation model to experimental data. Beyond that the focus will be on how different instrument settings can effect the energy resolution in some specific cases.

A better understanding of the energy resolution is essential to our understanding of the systems we study, since the certainty of our understanding is correlated to the precision of our measurements. This is relevant for all types of condensed matter systems measured with TAS.

2 Neutron Scattering

In this section the most relevant principles and equations of neutron scattering is explained, so as to give a better understanding on how the CAMEA instrument works. Section 2.1 is based on the lecture notes [8].

2.1 Scattering Theory

Because of quantum mechanics matter, and thus the neutrons, have both particle- and wave- like nature. One of the consequences of this is that the neutrons interact and scatter in correspondence to their wavelike nature, and the elastic scattering angle from scattering from a periodic structure such as a crystal can be determined through Braggs law

$$n\lambda = 2dsin(\theta). \tag{2.1}$$

Where n is the order of scattering, θ is the scattering angle, λ is the neutron wavelength and d is the lattice spacing between the scattering planes.

When measuring with neutrons, we are measuring in the Fourier transformed space known as reciprocal space. The neutron wave vector is given by $|\hat{k}| = \frac{2\pi}{\lambda}$, where λ is the wavelength. The momentum is given by $\mathbf{p} = \hbar\mathbf{k}$. The scattering vector $\mathbf{q}$ is defined by the difference in wave vector for the neutrons before and after scattering.

$$\mathbf{q} = \mathbf{k_i} - \mathbf{k_f} \tag{2.2}$$

The relation between the lattice spacing and the placement in reciprocal space for Bragg scattering, described by the $\mathbf{q}$ vector, is related by,

$$d = \frac{2\pi}{|\mathbf{q}|}, \tag{2.3}$$

as also depicted on figure 1. This drawing shows how to generate a certain $\mathbf{q}$-vector, based on the initial and final wave vectors that occurs when the neutrons scatters. Therefore one can control where in reciprocal space one measures by determining the scattering angles of the neutrons.

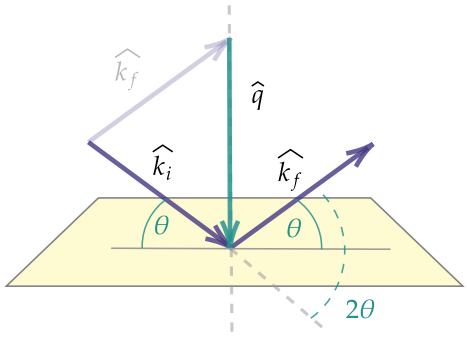

Figure 1: Illustration of scattering process with the incoming and outgoing wave vectors $\hat{k}_i$ and $\hat{k}_f$ and how they form the scattering vector $\hat{q}$.

In the case that $\mathbf{k_i}$ and $\mathbf{k_f}$ has the same length, the in going (E_i) and the outgoing energies (E_f) are also the same, since neutron energy relates to the length of the wave vector through the expression, $E = \frac{p^2}{2m_n} = \frac{\hbar^2 k^2}{2m_n}$. Therefore if one wants to measure inelastic scattering, the wave vector have different lengths. Thereby the energy difference can be determined,

$$\Delta E = \hbar\omega = E_i - E_f = \frac{\hbar^2(k_i^2 - k_f^2)}{2m_n}. \tag{2.4}$$

These are the central concepts needed to understand TAS instruments. The CAMEA instrument however takes these principles and adds on more complexity. Therefore I will in this project not look into resolution results for inelastic scattering, but focus only on the elastic resolution that is more easily described and measured.

2.2 CAMEA Instrument

The CAMEA instrument is a multiplexing TAS created for wide mapping of excitations, with the possibility for many types of extreme sample environments such as dilution refrigeration and strong magnetic fields. Multiplexing is a concept for TAS where multiple $(\mathbf{k_f}, E_f)$ are accessed to gain a

wider range in $(\mathbf{q}, \omega)$. CAMEA and Multi-FLEXX differentiates themself from previous versions of multiplexing spectrometers such as RITA-2, because instead of having in-plane scattering throughout the instrument, the secondary spectrometer uses vertical scattering.

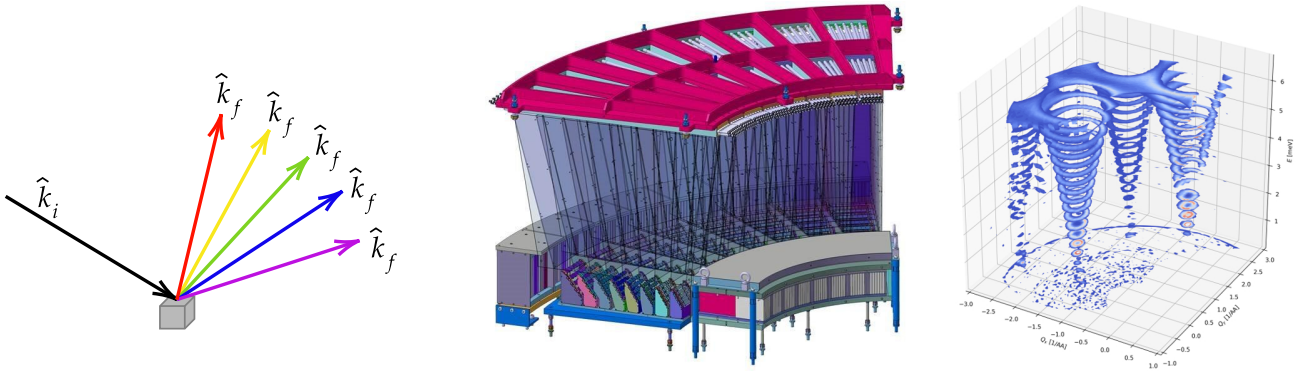

(a) **(b)**

Figure 2: (a) Illustation of the effect of mosiacity on the scattered neutrons. The neutrons at different energies can scatter in different angles mosiacity because of the differences in the angles of the small crystalites in the pyrolytic graphite. (b)(*left*) Schematic of the CAMEA detector tank, showing the berylium filter and the analyzer wedges scattering upwards into the detector-tubes. (b)(*right*) example of how CAMEA can measure dispersions in reciprocal space, both in multiple q-directions and as a function of energy. Picture provided by, the CAMEA instrument team.

Previously the in-plane scattering has lead to complex setups, strongly limited by spacial geometry. By rotation of the backend spectrometer to use vertical scattering, a lot more freedom is gained. Both is it possible to have multiple analyzers at different scattering angles, 2θ, from the sample, it is also possible to have multiple different energy analyzers for each of the 2θ angles. Thus we can measure many different outgoing wave vectors simultaneously. On figure 2b it can be seen how this concept is utilized for the CAMEA instrument. Here 8 different energy pyrolytic graphite (HOPG) analyzers are placed in succession, each set to scatter a certain energy of neutrons, from the lowest of 3.2meV to the highest of 5meV [3]. These analysers scatters vertically upwards into position sensitive half-inch detector tubes filled with ^{3}He and Ar. A set of 8 energy analyzers with the corresponding 13 detector tubes make out one wedge in the backend of the instrument. A total of 8 similar wedges are placed in at different 2θ angles to make the data acquisition even faster [9].

The analyzer crystals are placed in a symmetrical Rowland geometry[10], where distance collimation improves the resolution function. A sketch of a symmetrical Rowland geometry can be seen on fig. 3 and it is the geometry that guide, monochromator, sample position and the sample position, analyzer and detector follows. The idea is to place the scattering crystals in such a way that all scattering angles are the same and that the distance from both S and D to the middle analyser is the same. If the distances are different it becomes an asymmetrical Rowland geometry. It is the symmetric geometry that both the analyzers and the monochromator is constructed after.

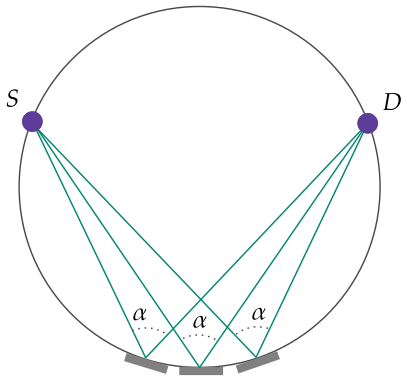

Figure 3: Illustartion of a symmetrical Rowland geometry. All the angles α are the same and from the middle analyzers to the both points S and D there is the same distance

2.3 The prismatic analyzer concept

The prismatic analyzer concept is possible because of the position sensitive detectors (PSD) and the mosaicity of the HOPG analyzer crystals. The mosaicity referes to the spread in the angles of small crystallites in the pyrolytic graphite. When scattering from a single crystal, a single $\hat{k}_f$ is scattered and the length of this is determined by the scattering angle. With moiacity there are many single crystals with different scattering angles in the material. This results that even though there is only one incoming wave vector $\hat{k}_i$, it can scatter many different $\hat{k}_f$ as shown on figure 6a. Pyrolytic graphite crystals can be purchased at specific outgoing mosaicity.

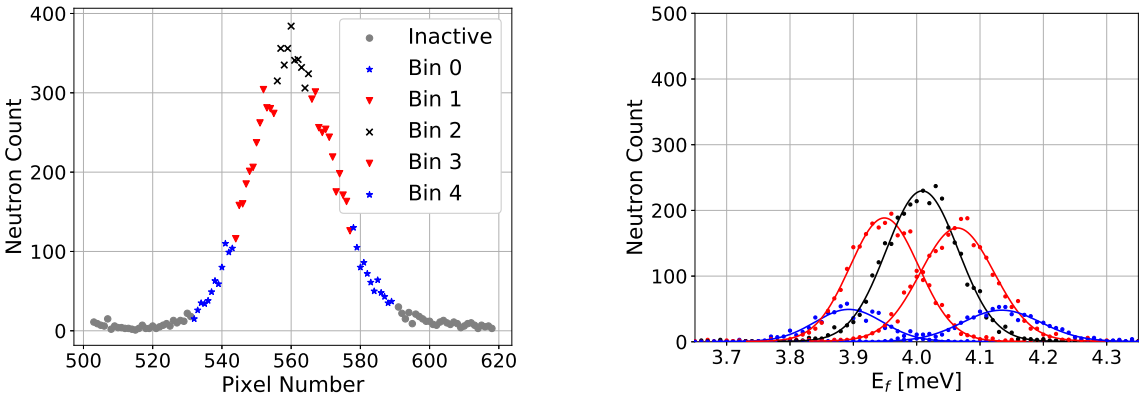

(a) **(b)**

Figure 4: from [9] (a) Signal for binning 1 as a function of pixel number. The red and blue dots shows how the pixels are divided into binning 5 (b) Measured and fitted energy dependence for binning 5.

The Rowland geometry of the analyzers, focuses the neutrons with a certain energy E_f into one point on the detectors, while neutrons with a slightly different E_f are focused at a different position because of the mosiacity of the analyzer crystals and the different Bragg angle. This creates focus points on the detector where neutrons are detected within a gaussian distribution for each energy. The prismatic concept is a way to measure multiple energies from the same analyzer, by splitting the active areas of the detector into multiple areas, thus binning the neutrons as visualized from figure 4a to 4b. This results in more energy distributions that all have a more narrow energy FWHM than the singled binned case.

The mosiacity is important for this concept to work, since it determines the energy width of the signal hitting the detectors. If the mosiacity is to small the signal will both be less intense and narrower, resulting in worse statistics for the binned data except for the central bin. On the other hand if it is to great, the signal will be too broad and overlap the neighboring detectors.

3 Energy resolution function

In this section we lightly explore the theoretical aspects of energy resolution theory, and put it into context of what we know so far about the energy resolution of CAMEA. The explanations included is to make the later results reproducible and to state the data treatment method.

3.1 Theory

When we theoretically consider neutrons scattering, we often approximate the TAS scattering as delta-functions meaning that we measure in a single point $\delta(Q - Q_0)\delta(\omega - \omega_0)$[8]. Due to divergence of the neutron beam, a resulting spread is experienced in both the momentum transfer and the energy distribution. The observed scattering is therefore a convolution between the resolution function $R(\mathbf{Q} - \mathbf{Q}_0, \omega - \omega_0)$ and the scattering function $S(\mathbf{Q}, \omega)$. To write an analytical expression for the resolution, the transmitted signal of collimators, monochromator and analyzer is approximated as gaussian functions in both $\mathbf{Q}$ and ω. The resulting resolution can be described from a 4-dimensional ellipsoid that changes shape both as a function of ω and $\mathbf{Q}$[1].

The most important expression we need for understanding CAMEA's resolution is the energy width, given as Full Width Half Maximum (FWHM), which can be determined from the resolution matrix M,

$$M = \begin{array}{c} \begin{matrix} q_x & q_y & q_z & E \end{matrix} \\ \begin{pmatrix} \multicolumn{3}{c}{\multirow{3}{*}{B}} & \multirow{3}{*}{J} \\ & & & \\ & & & \\ \multicolumn{3}{c}{J^{-1}} & C \end{pmatrix} \end{array} \begin{matrix} q_x \\ q_y \\ q_z \\ E \end{matrix}$$

Here, the FWHM of the energy is[11]

$$FWHM_E = 2\sqrt{2log(2)}(J^T \cdot B^{-1} \cdot J - C)^{-\frac{1}{2}} \tag{3.1}$$

The analytical calculations of the resolution functions are long and complicated and highly sensitive to changes in the experimental setup, making it impossible a to determine a full analytical expression for the dozens of types of instrument that exists. However, as is the case for this project, it can be estimated through numerical methods. With McStas it is possible to determine the resolution ellipsoid. An example of one of these simulations can be seen on fig. 5.

Since the FWHM as a function of energy is the parameter we want to estimate, we should to know the uncertainty for that parameter. To do this it will require to use the error propagation formula on Eq. 3.1. which, because of the co dependence of the cross terms is a non-trivial task and is beyond the scope of this project. Therefore the results in the later section will not include the uncertainty in the FWHM.

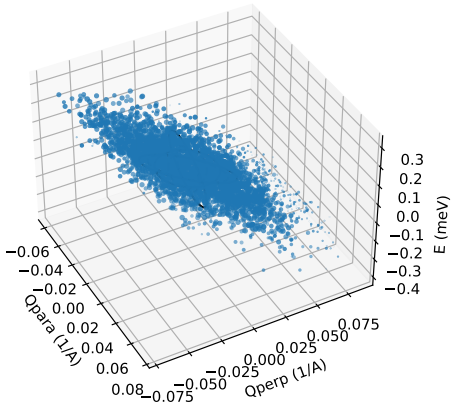

Figure 5: Example of an resolution ellipsoid, simulated in McStas for the CAMEA instrument and plotted with the *mcresplot* function.

4 McStas

McStas is a Monte Carlo ray-tracing package, used for simulating neutron instruments. It was first developed in the late 1990's and the community and contributions to the program has increased ever since.

McStas simulates *rays* of neutrons, where each ray represents multiple neutrons, since the neutron count in real experiments can reach a rate of $10^{15} n/s$ and is significantly more that modern computers can handle. Therefore each component treats the rays with a scattering probability modifying the mean neutron number or weight factor of the ray, as it passes through the virtual instrument[12].

4.1 Setup of CAMEA McStas Model

As described in 2.2, CAMEA is a highly complex TAS instrument with 8 wedges of analyzers and detectors measuring at multiple energies. It consists of 104 PSD-detectors and hundreds of analyzer crystals, all having a unique placement and rotation.

For the purpose of making an effective model, a previous McStas model was used as the skeleton for the resolution modeling. The model used is the one developed by Jakob Lass in 2018 and includes the updated focusing guide installed at PSI in 2019 as well as the option to simulate both the new and the old monochromator. The new monochromator was installed in October 2021.

The virtual instrument was modified so that instead of simulating all 8 backend wedges, only one was kept, significantly decreasing computation time. To determine the resolution we look to the work by Cooper and Nathans who determined that the intensity, I, observed in a neutron experiment is given by[13]

$$I(Q_0, \omega_0) = \int R(Q_0 + \Delta Q, \omega_0 + \Delta\omega)\sigma(Q_0 + \Delta Q, \omega_0 + \Delta\Omega)d(\Delta Q)d(\Delta\omega), \tag{4.1}$$

where σ is the scattering cross section and R is the resolution function given by the transmission probability ,$P(Q, \omega, path)$, and then integrating that over all possible neutron paths.

$$R(Q, \omega) = \int_{path} P(Q, \omega, path). \tag{4.2}$$

In work by Lefmann et al. [7], this was converted into a Mcstas component pair consisting of a sample and a monitor. As mentioned above the neutrons weight is calculated and this is proportional to the transmission probability. This allows a Monte Carlo integral over all paths Eq. 4.2 for the choosen Q and ω. The *res_sample component* has a constant scattering cross section $\sigma(Q, \omega)$ and the *res_monitor* determines the resolution function monotoring the actual (Q, ω) scattered by the neutron when the instrument is set up to observe $_0$, ω_0.

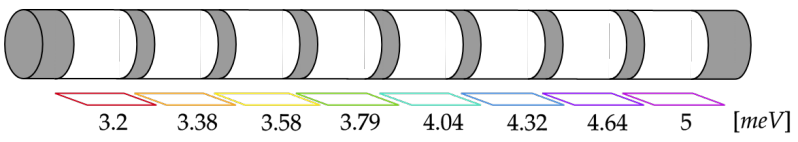

Figure 6: Illustration of how the resolution monitors in binning 1 setting is placed just below the active areas the detector tube in the McStas model.

For the McStas model of CAMEA, the *res_sample* is located at the sample position previously defined in the simulation. Multiple *res_monitor*s are placed in correspondence with the active areas of the pixels of the detector-tube defined for binning 1, see fig. 6, meaning one monitor for each analyzer.

5 Results and Discussion

In this chapter, a series of different results are presented. These particular test were performed to solve some of the unanswered questions that was current for the CAMEA instrument team at the time of this project, but it also come to show the versatility of the McStas model. All simulations were performed with a sample size of h=0.015m and cylinder radius of 0.01m

5.1 Previous measurements of the energy resolution

To validate and compare the results from the McStas model, we look at previous measurements from the instrument setup with the old non-focusing guide. The resolution was also determined with experiments and simulations. The old results of the elastic energy resolution is showed on fig. 7.

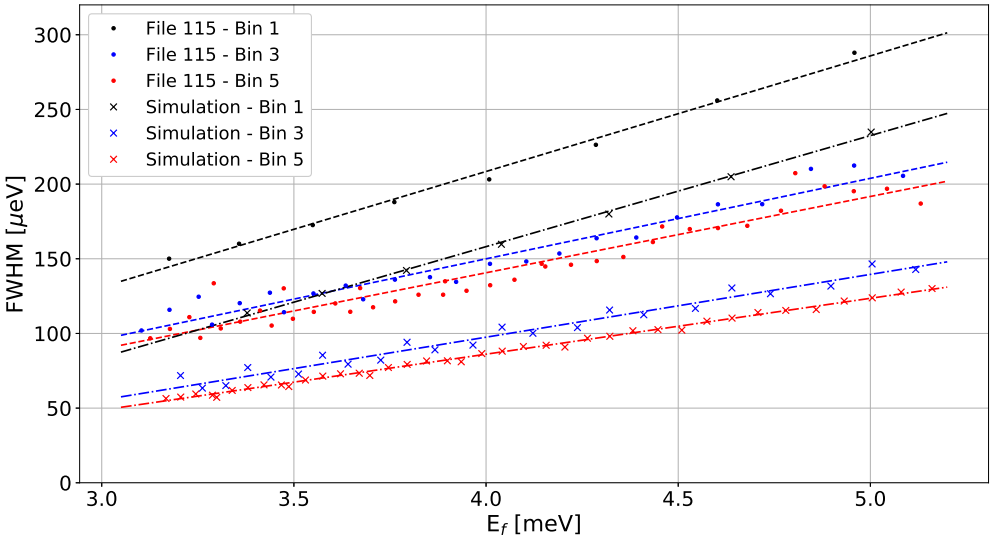

Figure 7: FWHM of the elastic energy resolution, showing both measurements and simulations for multiple binnings. picture from [9].

It is clear that there is a linear dependence of the FWHM with the final energy E_f but a discrepancy between experiments and simulations. For the simulation points on this graph, not all of the instrument was simulated. They are the resolution points from the backend of the spectrometer, found by simulating a source at the sample position, through a vanadium scan, showing that the backend has a better energy resolution than the primary spectrometer. The data also shows that a significant increase can be made in the energy resolution by using the prismatic concept and changing the binning. This will work as a frame of reference for the results from our simulation.

5.2 The new and old monochromator

We want to validate that the monochromator component works as intended and to see if there is any energy resolution effects. In fig. 8, a comparison is seen between energy spread the old vertical-focusing and the new double-focusing monochromator simulated at the end of the focusin guide. Figure (a)

show a scan of all 8 elastic energies for both mono-setting. It is clear that there is a significant increase in the intensity with an approximate factor 3.5 increase for the $3.2meV$ monitor. A rough estimate of change in the between the resolution is made by fitting a gauss, though the function is not entirely gaussian, to the two $5meV$ signals, as seen on fig. 8b. With a FWHM of $0.08111meV$ for the old and $0.08109meV$ for the new mono, there is hardly any difference that is visible in an experiment. This is reasonable since the mono is already in a Rowland geometry and that the focusing only affects the reflectively of the blades.

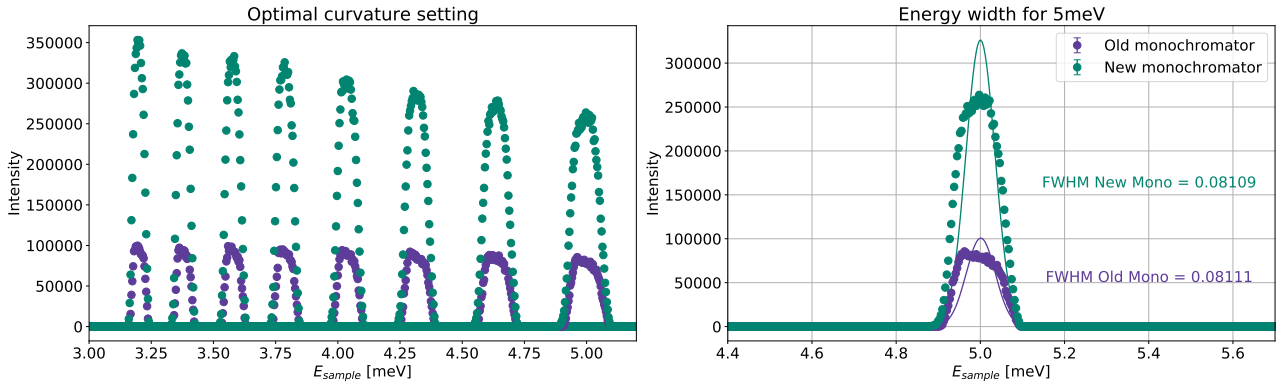

(a) **(b)**

Figure 8: (a) Comparison of the new(green) and old(purple) monochromator intensity at the sample position for the elastic signals for binning 1 (b) width of the 5meV signal at the sample position with fitted curves with FWHM.

When testing the simulation, it was found that the curvature of the monochromator was wrong with a factor of 2. This was found by scanning over the *RH_bool* and *RV_bool* variables in the McStas file, were 1 is the previous value used to "turn on" the focusing in either horizontal or vertical direction, the optimal value was found to be at 0.5. Comparison between the previous setting of 1 and the optimal value of 0.5 can be seen in appendix A.

5.3 Comparison between middle and edge detectors

The original purpose of creating a resolution function McStas model of CAMEA, was to investigate whether there was any difference in the energy resolution compared to where on the wedge the scattered neutrons hit. To estimate any difference two sets of *res_monitor*s were placed as shown on figure 6 for both the middle and edge detector in the wedge as shown on fig. 9.

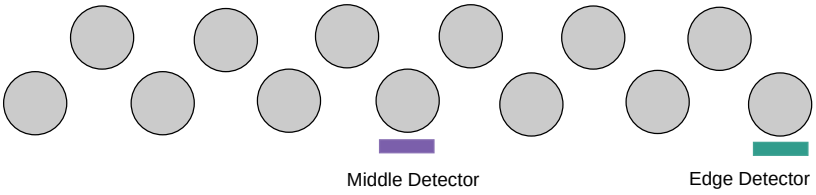

Figure 9: Illustration of a cross section of a detector wedge, and how the *res_monitors* are placed relative to the detector tubes.

Because the simulations were done over an initial energy range E_i that does not have equal step size between each initial energy E_i, a simulation scan in McStas can not be performed. The entire simulation therefor have to be redone for each of the energy settings in E_i to simulate all the elastic

energies. This has been done in a Bash script to automatize the process. The edge and middle resolution results can however be found at the same time for each initial energy E_i simulation, as a there can be multiple *res_monitors* related to the same *res_sample*.

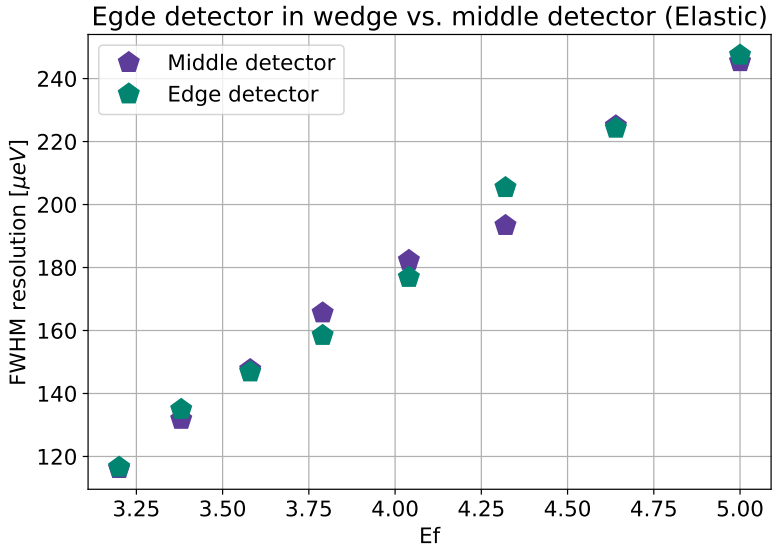

Figure 10: Simulation results showing the difference between the middle and edge detectors FWHM for each of the elastic final energies.

The results in fig. 10 have almost perfectly overlapping data points that has a linear dependence very close to the results from fig. 7 simulation of bin 1. This gives a clear indication that there is no significant difference in the energy resolution between the middle and edge detectors in a wedge.

5.4 Virtual source slit

The virtual source slit is an adjustable slit that is placed at the beam focus point after the guide opening. By narrowing the slit, the divergence of the beam at each PG blade in the mono is diminished in turn improving the resolution at a cost in flux. With the installment of the doubly focusing monochromator, the energy resolution for different slit settings were measured to see if there was anything significant to gained in the energy resolution. The results respectively for the experiment and simulation of the same settings are shown on fig. 11 a and b.

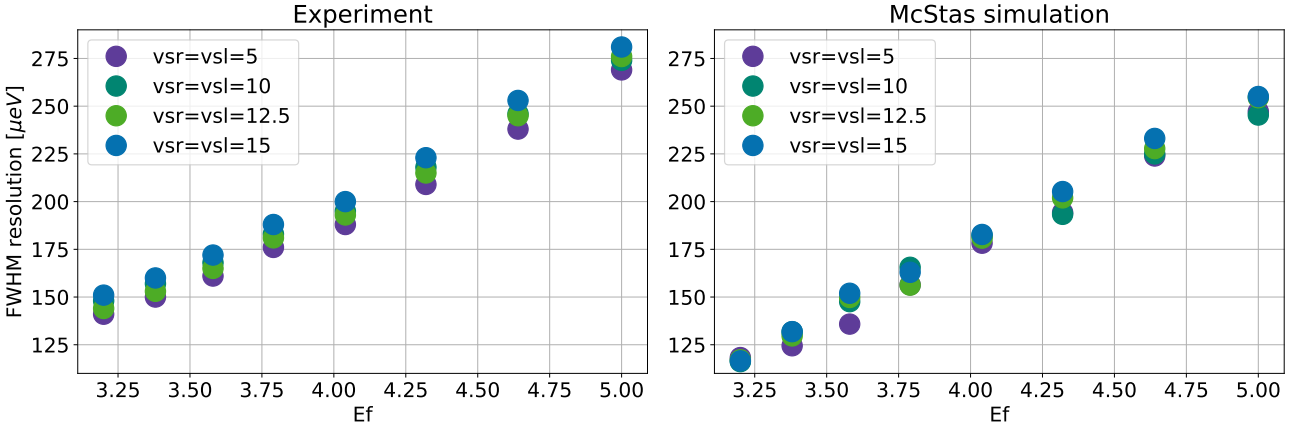

Figure 11: (left) the experimentally measured FWHM for the elastic binning 1 energies for different virtual slit setting. (right) simulation of the same virtual slit settings, showing the overall same trend but with an negative offset relative to the measured data. All *vsl* and *vsr* values are in [mm] and the y-axis are set to the same ranges for both plots to more easily compare the results.

Comparison between the experimental data and the corresponding simulation for setting of the

left and right slit (vsl=vsr), can be seen in appendix B. We can see there are __ similarities in the two results, both experiment and simulation follow a linear trend and both do not have a any major differences in the energy resolution for the different slit settings. The main difference being in the offset between the two lines. An explanation for this might be that the simulation is an idealized model of the spectrometer, while in the real world, small wrong adjustments are more prone to happen, therefore increasing the resolution slightly in the experimental results.

The fluctuations in the simulation results are probably due to a lack of statistics and could likely be improved with longer run time. The small change in resolution with slit setting could indicate that the instrument resolution is dominated by the analyzer. Therefore these tests should be repeated by a higher binning value.

5.5 Placement of virtual source

Another parameter that is considered to maybe have and effect on the energy resolution is the placement of the virtual guide slit after the end of the focusing guide.

In the McStas model a functionality was added so that it became possible to map out the neutron beam after the guide opening. A movable PSD monitor is included with an initial setting variable, *psd_dist*, that determines its distance from the opening of the guide. The detector is wide enough so that it shows the majority of the beam up to a distance of 1.5 m which is in most cases sufficient as the monochromator is placed 1.6 m from the opening of the guide. This distance is equal to the mono-sample distance. A total two-dimensional horizontal cross section of the beam is found by taking the middle row in height of pixels in the PSD detector and plotting that as a function of the *psd_dist*, see fig. 12b.

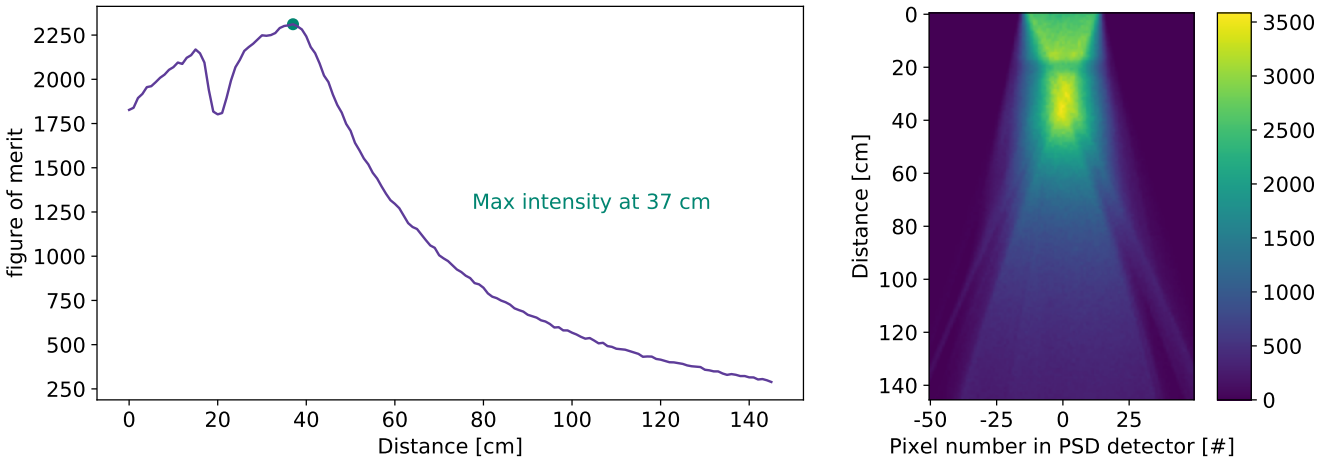

Figure 12: (a) figure of merit showing average weighted intensities of position sensitive detector (PSD) signal as a function of distance from the guide opening. (b) Cross section of the beam signal at the middle of the PSD monitor as a function of distance from the guide opening.

To estimate the focus point, a weighted mean for each of the pixel rows in fig. 12b are calculated using

$$A = \frac{\sum_i pixel\_count_i \cdot weight_i}{\sum_i weight_i}, \tag{5.1}$$

where the weights are given as $weight_i = |pixel\_count_i^{-1}|$ and the neutron count in pixel zero is set to $weight = 1$. This is not representative of any physics, it is merely a method to estimate where the beam is most focused. The weighted average, A, is plotted as a function of distance, as seen on fig. 12a. The maximal value is found to be 37 cm from the opening of the guide also corresponding to the most narrow point on fig.12b. This is expected from the guide focusing. It has not been possible to explain or further investigate the unphysical dip and the corresponding stripe that can be observed around 20 cm. An idea for further investigation, is to use the the 2D UNION Monitor and position it in the scattering plane to get another visualisation of the beam and its surroundings.

The finding that the focus point of the beam sits approximately 37 cm after the guide, made cause for concern. The front end spectrometer is supposed to be in a symmetric Rowland geometry which depends on that the distance from mono to guide and mono to sample are the same. The simulations however indicate that the focus point, where the Rowland geometry works from is only 123 cm from the mono, making one side of the geometry 37cm shorter than the other, making it a asymmetric Rowland geometry instead. After checking with the simulation and the technical drawings for the instrument, this indeed seem to be the case and that I have found a construction error in the CAMEA instrument. Further investigations with more simulations will have to made to estimate the effect of this mismatch in the Rowland distances.

5.6 Outlook

Throughout this project I have developed a McStas model that is optimized for investigating instrument parameters and the effect of those parameters on the energy resolution function. There is, however, still a lot of work that can be continued with this simulation model. One of the first major things is as mentioned in the previous section, the placement of the focus point relative to the monochromator and the virtual guide slit which is a potential mistake in the instrument design/construction. Further simulation work should include results of the energy resolution function for different placements of the the virtual slits as well should a simulation be performed where the monochromator and backend is moved to fulfill a symetric Rowland geometry, that is to see if any reconstrution of the instrument will pay off in regards the improvements of flux, resolution and resolution with a higher binning.

It would be nice to do a more in depth analysis and comparison of the monochromator curvature to see if the improved curvature corresponds with the one found experimentally.

Since the model is a full instrument, there are endless parameters that can be investigated further. The sample size used is another interesting feature since it is a scattering component, it effects the resolution just like the other instrument components. Therefore scanning resolution for different sample sizes is relevant especially for the users, so they have a better idea of the resolution they can achieve with their samples and optimize their experiment after it.

These propositions for test have the common theme that they are for elastic energies. The next step, that is possible because of the *res_sample* and *res_monitor*, is to investigate the resolution function for inelastic scattering. This could open up to whole new insights into how the instrument works.

References

[1] G. Shirane, S. M. Shapiro, and J. M. Tranquada. *Neutron Scattering with a Triple-Axis Spectrometer*. Cambridge University Press, Cambridge, 2002.

[2] Bertram N. Brockhouse. Slow neutron spectroscopy and the grand atlas of the physical world. *Rev. Mod. Phys.*, 67:735–751, Oct 1995.

[3] Felix Groitl, Dieter Graf, Jonas Okkels Birk, Márton Markó, Marek Bartkowiak, Uwe Filges, Christof Niedermayer, Christian Rüegg, and Henrik M Rønnow. Camea—a novel multiplexing analyzer for neutron spectroscopy. *Review of scientific instruments*, 87(3):035109–035109, 2016.

[4] Prismatic analyser concept for neutron spectrometers. *Review of scientific instruments*, 85(11):113908–113908, 2014.

[5] Felix Groitl, Rasmus Toft-Petersen, Diana Lucia Quintero-Castro, Siqin Meng, Zhilun Lu, Zita Huesges, Manh Duc Le, Svyatoslav Alimov, Thomas Wilpert, Klaus Kiefer, Sebastian Gerischer, Alexandre Bertin, and Klaus Habicht. Multiflexx - the new multi-analyzer at the cold triple-axis spectrometer flexx. *Scientific reports*, 7(1):13637–12, 2017.

[6] P.G Freeman, J.O Birk, M Markó, M Bertelsen, J Larsen, N.B Christensen, K Lefmann, J Jacobsen, Ch Niedermayer, F Juranyi, and H.M Ronnow. Camea ess – the continuous angle multi-energy analysis indirect geometry spectrometer for the european spallation source. *EPJ Web of conferences*, 83:3005–, 2015.

[7] K Lefmann, K Nielsen, A Tennant, and B Lake. Mcstas 1.1: a tool for building neutron monte carlo simulations. *Physica. B, Condensed matter*, 276:152–153, 2000.

[8] Kim Lefmann. Neutron scattering: Theory, instrumentation, and simulation, 2019. Lecture notes: University of Copenhagen.

[9] J. Lass et al. Design and performance of the multiplexing spectrometer camea. 2020. arXiv:2007.14796.

[10] Markos Skoulatos, Klaus Habicht, and Klaus Lieutenant. Improving energy resolution on neutron monochromator arrays. *Journal of physics. Conference series*, 340(1):12019–, 2012.

[11] Jakob Lass. Camea data analysis: a data treatment software package, 2017. Master Thesis.

[12] Peter Kjær Willendrup and Kim Lefmann. Mcstas (i): Introduction, use, and basic principles for ray-tracing simulations. *Journal of neutron research*, 22(1):1–16, 2020.

[13] M. J Cooper and R Nathans. The resolution function in neutron diffractometry. i. the resolution function of a neutron diffractometer and its application to phonon measurements. *Acta crystallographica*, 23(3):357–367, 1967.

Appendix A

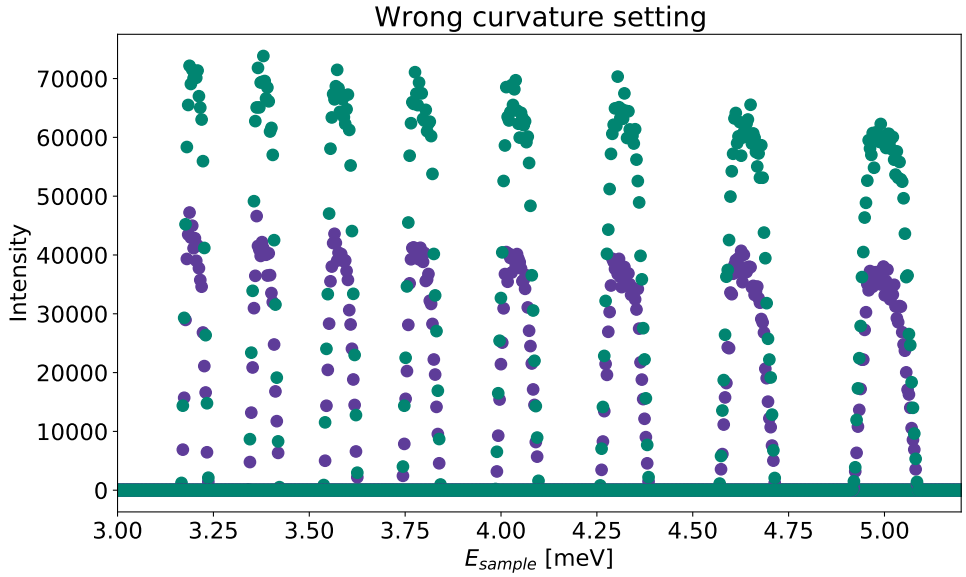

(a)

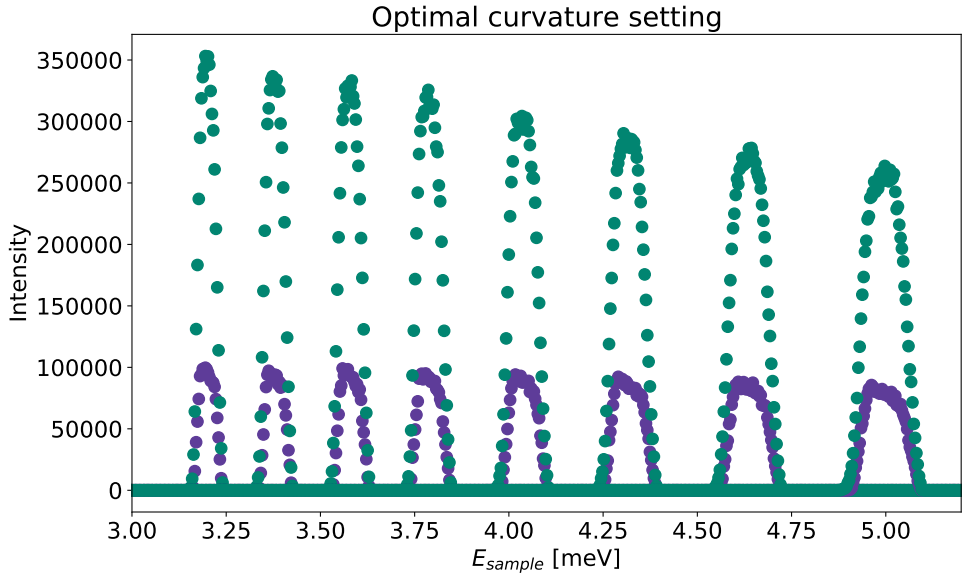

(b)

Figure 13: Comparison of the previous monochromator curvature (top) where *RV_bool* and *RH_bool* values were 1 for both the new and old mono setting and the optimal curvature (bottom) with a *_bool* value of 0.5. Settings were wrong for both the new and the old mono settings since they use the same function(s) to calculate the curvature.

Appendix B

Comparison of simulation and experiments

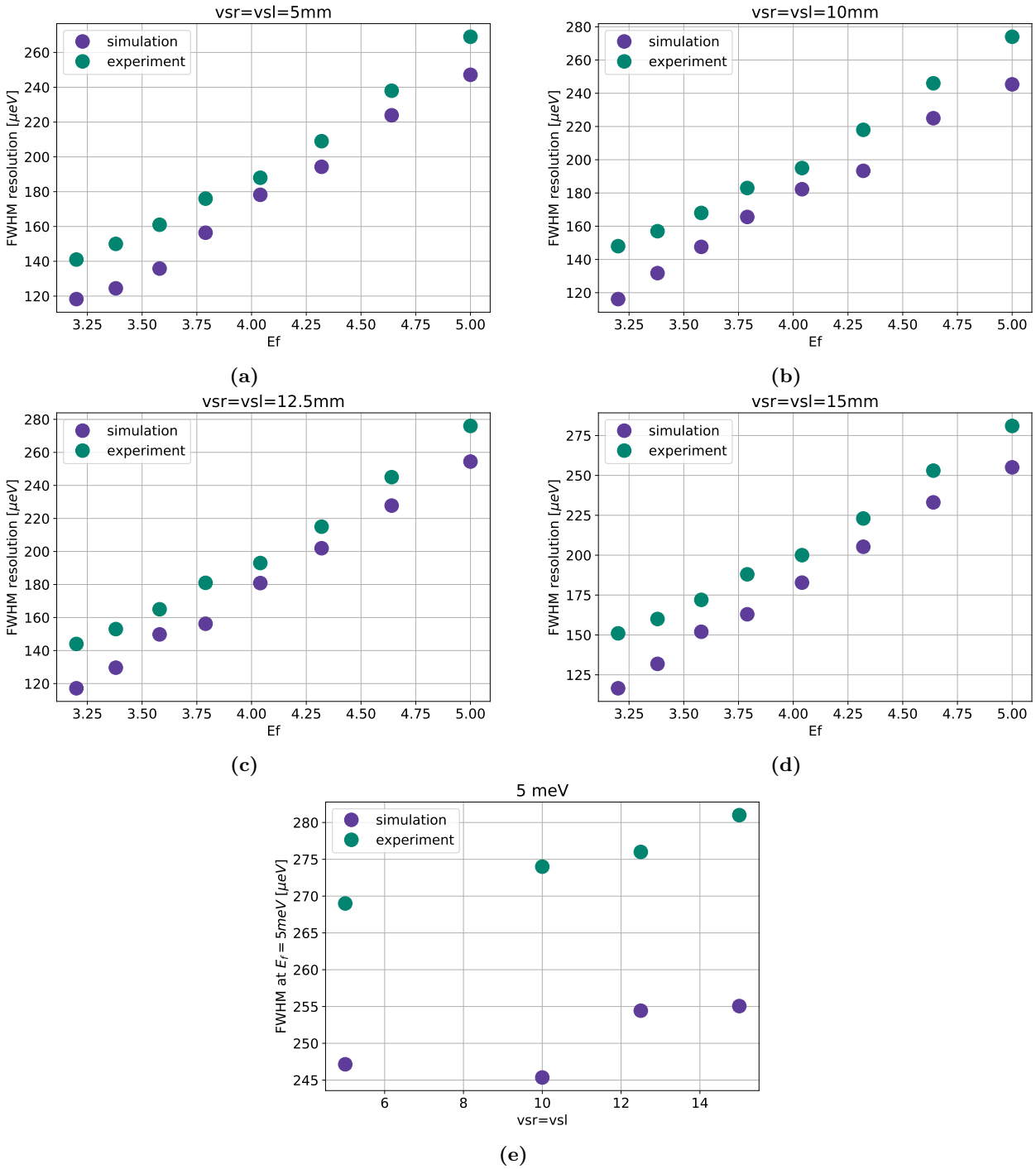

Figure 14: Comparison of the simulation and experimental resolution for each of the different virtual source settings (e) shows the FWHM as a function of the virtual source settings for the 5meV elastic signal